Chapter 6

Spark Plasma Sintering of Zirconia-Toughened Alumina Composites and Ultra-High Temperature Ceramics Reinforced with Carbon Nanotubes

Ipek Akin[*1], Gultekin Goller[2]

[1,2]Department of Metallurgical and Materials Engineering, Istanbul Technical University, 34469 Maslak Istanbul, Turkey

[*1]akinipe@itu.edu.tr; [2]goller@itu.edu.tr

I. INTRODUCTION

The most commonly accepted definition of ceramic is a refractory, inorganic, and non-metallic material with essential components [1, 2]. Ceramics are capable of withstanding high temperature as high as 2000 ℃. They have high melting temperature, and good mechanical properties including hardness, compressive strength, and Young's modulus [3]. Ceramics have different characteristics, which enable them to be used in a wide variety of applications from bricks and tiles to leading edges of hypersonic vehicles. The properties of ceramic materials are dependent on the type and strength of bonding (ionic and/or covalent), the arrangement of atoms (amorphous or crystalline), the way of atoms packing, chemical composition, and microstructure.

In the light of these parameters, ceramics are classified as traditional and advanced (engineering or technical) ceramics. The raw materials of traditional ceramics are mainly silica or clay based [2, 3]. Traditional ceramics include consumer products such as earthenware, stoneware, porcelain, construction materials (e.g., brick and tile, cement), refractories, tableware, and sanitary wares. On the other hand, the raw materials of advanced ceramics are chemically prepared high-purity powders, and generally more expensive and complex processing routes are applied for the production of them. Generally, they have superior corrosion resistance, good wear performance and unique mechanical, thermal, optical, electrical and magnetic properties. Examples of advanced ceramics include bioceramics (Al_2O_3, YSZ: yttria stabilized zirconia, hydroxyapatite, Bioglass®, etc.), electroceramics (piezoelectrics, pyroelectrics, dielectrics, $BaTiO_3$ and $SrTiO_3$ for capacitors, ZnO for varistors, SnO_2 as gas sensors, etc.), nuclear ceramics (BeO, UO_2, etc.), armour ceramics (B_4C, SiC, etc.) [4, 5], and thermal protection systems (Al_2O_3, YSZ, ceramic tiles, etc.).

Advanced ceramics are utilized at specific applications that demand high performance [6]. Based on their properties, advanced ceramics are further classified as structural and functional ceramics. Applications of structural ceramics are aimed to optimize mechanical properties, basically fracture toughness, hardness, strength, Young's modulus, wear resistance, and as well as oxidation behaviour. On the other hand, functional ceramics are related to the optical, electrical, and magnetic properties [3].

Besides, it is possible to make an additional classification for structural advanced ceramics based on their composition as oxides (Al_2O_3, TiO_2, MgO, ZrO_2, etc.) and non-oxides such as carbides (SiC, B_4C, ZrC, TiC, etc.), borides (HfB_2, ZrB_2, TiB_2, NbB_2, etc.) and nitrides (Si_3N_4, AlN, TiN, BN, etc.).

A. Importance of CNTs as Reinforcing Phase for Ceramic Matrices

Ceramic matrix composites (CMCs) are subgroup of engineering ceramics. They involve ceramic matrices in which, ceramic may form the matrix, reinforcement, or both. The concept of CMCs has been developed to overcome brittleness of monolithic engineering ceramics. Accordingly, one of the main reasons for producing ceramic matrix composites is to improve mechanical properties. Moreover, they can be utilized at elevated temperatures due to their high temperature stability and good corrosion resistance. However, low fracture toughness of ceramics and ceramic matrix composites make them unsuitable for some specific applications. Several techniques have been developed to improve fracture toughness of ceramics by incorporation of additives including particles (SiC, etc) and fibers (C, SiC, etc.). For instance, it was reported that, addition of SiC nanoparticles into Al_2O_3 altered the fracture mode of Al_2O_3 from intergranular to transgranular. As it is known, this transition can be interpreted as improved strength and toughness in ceramics. Second phase additions can enhance grain boundary properties (i.e. grain size refinement) and activate several toughening mechanism including crack

deflection, crack bridging, etc. [7, 8].

In the past few decades, single, double or multi-wall carbon nanotubes (CNTs) have received an increasing scientific importance due to their remarkable properties originating from their unique structure. The combination of superior physical, mechanical (elastic modulus >1 TPa, tensile strength >150 GPa), electrical (conductivity >1.5 x 10^4 S/m) and thermal (conductivity >2000W/mK) properties makes CNTs one of the most preferred reinforcing materials for engineering ceramics and composites. The large aspect ratio of CNTs enhances load transfer with the matrix and provides effective reinforcement. In addition, the superior flexibility of CNTs improves fracture toughness of ceramic matrix composites.

Over the last two decades, different composite materials have been produced by incorporation of CNTs as toughening and reinforcing agent into a metal (e.g. Al, AZ91D and AZ31 Mg alloys, Ti, Cu, Ni, Co, Fe, etc.), ceramic (e.g. mostly Al_2O_3, Al_2O_3-ZrO_2, ZrO_2, Fe-Al_2O_3, FeCo-$MgAl_2O_4$, SiO_2, TiO_2, SiC, Si_3N_4, B_4C, ZrB_2, TaC, etc.) or polymer (e.g. polysulfone, PEEK, PLA, PGLA, etc.) matrices [7, 8]. CNT-reinforced systems can be used for a wide range of applications including aerospace vehicles, commercial aircraft, manned or unmanned aerial vehicles, satellites, space launch vehicles, hydrogen storage encapsulation, lightning protection for aircraft, military applications, and electrical industry with improved mechanical, thermal and wear properties. In addition, CNTs have been investigated for potential biological applications (such as drug delivery and biosensors) due to their excellent chemical stability, high surface area, and acceptable biocompatibility. CNTs have also been utilized for some applications including tissue regeneration, gene and immune therapy [7].

The purpose of this chapter is to summarize a series of spark plasma sintering (SPS) experiments conducted on multi-wall carbon nanotubes (MWCNTs) reinforced zirconia toughened alumina (ZTA) composites and ultra-high temperature ceramics (UHTCs) based on both transition-metal diborides (ZrB_2 and ZrB_2-SiC composites) and carbides (ZrC-TiC, ZrC-SiC composites).

The present chapter is divided into three main sections: (i) Section II deals with the CNT-reinforced ceramic matrix composites including dispersion characteristics, densification of ceramics with CNTs additions and characterization; (ii) Section III is dedicated to spark plasma sintered zirconia toughened alumina (ZTA) composites reinforced with carbon nanotubes (CNTs), and (iii) Section IV is focused on the spark plasma sintered ultra-high temperature ceramics having CNTs as a second or third phase. Emphasis is placed on densification behaviour, mechanical properties and microstructural development of the composites having different amounts of CNTs in the following sections.

II. CNT-REINFORCED CERAMIC MATRIX COMPOSITES

A. Dispersion of CNTs in Ceramic Matrices

One of the most important problems in processing of CNT-reinforced composites is inhomogeneous dispersion of CNTs within the matrix and formation of CNTs clusters. CNTs tend to form agglomerates due to their high surface area, geometry, and van der Waals forces. Problems such as inadequate densification, weak bonding interfaces between CNTs and matrix grains, lack of toughening, formation of defects and stress-concentration zones emanate from inhomogeneous dispersion of CNTs and formation of agglomerates [8, 9].

Homogeneous distribution of CNTs has a significant role in achieving desired mechanical properties and attains a good balance with other properties of ceramics (e.g. surface quality, electrical and thermal conductivity, etc.). In such a case, individual CNTs can carry load and contribute toughening mechanisms with crack bridging and pull-out effects [9, 10].

To achieve a good dispersion of CNTs in ceramic matrices, appropriate batch preparing and processing routes should be performed.

The CNT-reinforced composite production route has two steps:

(i) Powder mixture preparation using an appropriate CNT dispersion technique,

(ii) Densification with appropriate pressureless or pressure-assisted sintering techniques.

Powder mixture preparation methods can be classified into three groups as follows:

(i) Mixing ceramic powder and CNTs, and colloidal mixing,

(ii) *In situ* synthesis of the ceramic in CNTs,

(iii) *In situ* synthesis of the CNTs in ceramic [11, 12].

Mixing ceramic powders with CNTs in wet media is one of the most widely used methods [12]. CNTs can be dispersed in ethanol with an ultrasonic probe. In our previous studies [13-16], two-stage distribution process was applied. In the first stage, ultrasonic homogenizer (Bandelin Sonopuls HD 2200, operating at 50% amplitude with on and off cycles) was used to disperse CNTs in ethanol. Then, the dispersed CNTs were mixed with matrix powder mixture slurry. In the second stage, CNTs were dispersed again with a more powerful ultrasonic agitation (Hielscher UP400S, operating at 50% amplitude with

on and off cycles). All compounds (in ethanol media) were stirred until most of the ethanol evaporated, and then the powder mixture was dried at 105 ℃ for one day in a drying oven. Sun et al. [17] used organic additive (polyethyleneamine, a kind of dispersant) to improve the dispersion characteristics of treated (in NH_3 at 600 ℃ for 3 h) MWCNTs in Al_2O_3 matrix. They applied ultrasonication for 30 min and reported an enhanced dispersion of treated MWCNTs.

In some studies, composite powders are prepared by the synthesis of the ceramic *in situ* around the CNTs. $BaTiO_3$-MWCNT, $NiFe_2O_4$-MWCNT and TiN-MWCNT composites are the examples of *in situ* synthesized oxides and nitrides having CNTs with better distribution characteristics than those obtained by mixing ceramic powder and CNTs.

The third method to prepare homogeneously distributed CNTs-ceramic composite powder is synthesis of CNTs *in situ* in ceramic powder by using combustion chemical vapour deposition (CCVD) technique. This synthesis method is carried out by the treatment of a ceramic powder which contains nano-sized catalytic metals (e.g. Fe, Co, Ni, etc.) in an atmosphere containing carbon monoxide or hydrocarbon at 600-1100 ℃. MWCNT-Fe-Al_2O_3, SWCNT-Co-$MgAl_2O_4$ and MWCNT-Co-MgO are the examples of composites synthesized by this method. Obviously, the composite powders contain both CNTs and metals [12].

B. Densification of CNT-Reinforced Ceramic Matrix Composites

The densification of CNT-reinforced composites includes pressureless sintering and pressure-assisted sintering techniques. It must be pointed out that, in all processing routes, nanotube integrity should be maintained during processing in order to achieve desired reinforcing properties [18].

Pressureless sintering is relatively economical and easy process. In essence, pre-consolidated ceramic powders are heated in a furnace under controlled atmosphere (such as argon, nitrogen, etc.) [7]. On the other side, the development of high-performance ceramic composites with fine-grained microstructure and significantly improved mechanical, optical, magnetic, thermal, and electrical properties by applying a pressure during heating the sample can be accepted as one of the most important developments in ceramic processing. The externally applied pressure during sintering is important to achieve full densification. Simultaneous application of pressure and temperature enhances the sintering process by contributing to sintering driving force. Mainly, there are two ways to apply external pressure during sintering: (i) uniaxial pressure (e.g. hot pressing, spark plasma sintering) and (ii) isostatic pressure (e.g. hot isostatic pressing) [6, 7].

Hot pressing (HP) has been commonly used to prepare samples having high density (low porosity) and enhanced mechanical properties. HP is limited to simple solid forms, but it is possible to obtain the sample with exact dimensions. Rectangular, square or cylindrical cross sections such as blocks and plates with high dimensional accuracy can be manufactured. In hot pressing, compaction under a uniaxial pressure (up to 80-100 MPa) and sintering of high-purity powder progress simultaneously between punches in a die. Graphite is the most widely used die material due to its low cost, high strength at high temperature (up to ~2200 ℃), good creep resistance, high thermal conductivity and relatively low thermal expansion. It is worth noting that atmosphere control at high temperature is usually required for hot pressing. For instance, an inert atmosphere (such as nitrogen, argon, etc.) should be used above 2200 ℃ because of the vapour pressure of graphite [2, 6, 7].

Hot isostatic pressing (HIP) uses the application of isostatic pressure during heating the sample. In the original HIP process (i.e. encapsulated method), the preformed powder is weighed into a deformable metal container and then exposed to pressure and heat to take desired shape. The green preformed compact is sealed in a glass envelope that could be stripped after hot isostatic pressing process. In other type of hot isostatic pressing (i.e. not encapsulated method), the pre-consolidated powder is sintered at a high temperature ~ 2000 ℃ in a furnace that can be pressurized up to ~ 200 MPa [2, 6, 7]. During heating, the sample is subjected to an increased gas pressure (mostly argon, reactive and oxidizing gases). The primary advantages of HIP process are producing dense materials without significant grain growth and capability for sintering samples with complex shapes (e.g. silicon nitride nozzles, alumina-based tool bits) and different geometric features due to homogeneous pressure distribution during process. The capability of HIP process for preparing products having irregular shapes gives several advantages in terms of applications and design flexibility [2, 6, 7, 19].

During the last twenty years, spark plasma sintering (SPS) or field assisted sintering technique (FAST), current-activated pressure-assisted, and pulsed electric current sintering (PECS) techniques have been developed as densification methods for producing dense materials at a relatively lower temperatures and in a shorter period of time compared to the conventional sintering techniques [7, 20, 21]. Actually, the history of plasma activated sintering methods dates back to the late 1930s with the development of sintering process using electrical energizing in United States. In the 1960s, a similar process based on a pulse current (known as spark sintering) was applied by Inoue et al. for sintering of the samples in Japan. However, the developments were very limited until the middle of 1980s and early 1990s. In 1990, Sumitomo Heavy Industries Ltd. developed the first commercial spark plasma sintering system. SPS is a third generation of the aforementioned technology with large pressures and direct current (DC) pulse generators of 10 to 100 tons and 1 to 30 kA, respectively [7, 22].

SPS is a uniaxial pressure-assisted synthesis and processing technique, which employs low voltage and high current

(pulsed direct current) from the beginning to the end of the sintering process under low atmospheric pressure. SPS seems to be similar to hot pressing (HP) method, but it is regarded as fast sintering method and heating mechanism, effects of electric field and electric current, and ways of heat transfer to the sample show differences. In the SPS technique, very high thermal efficiency can be achieved. The sample and die-punch rod assembly (mostly graphite) are directly heated with a pulsed direct current (DC) which passes through graphite punch rods, powder and dies simultaneously under a uniaxial pressure. Typically, external heating elements are not used in a conventional SPS system. Heating is achieved by way of a pulsed (on/off) DC. Moreover, application of on/off direct current generates spark plasma, Joule heating and an electrical field diffusion effect. In addition, on/off DC current form local high temperature states (several to ten thousands ℃), and cause vaporization and melting of the powder surfaces and promote sintering. This induces enhanced neck formation around contact area and improved densification [7, 20-22]. However, it is worth to note that, the generation of plasma during SPS process is still a controversial issue.

The electrical conductivity of the material is important for heat transfer mechanism in SPS process. If the pre-consolidated powder is conductive (e.g. metal powders), the current mainly flows through the sample and a small portion flows through the die. In the case of insulating powders (e.g. alumina, zirconia, etc.), heat is produced by Joule heating and efficiently transferred to the sample [7, 22].

Processing of CNT-reinforced composites in high relative densities without damaging the CNT structure is a challenging issue. Although the application of pressure can damage the CNT structure, SPS is one of the most efficient techniques to achieve complete densification without damaging the structure of CNTs [12]. In hot pressing (HP) method, heating up the system and heat transfer from chamber atmosphere to the die (or sample) takes longer time when compared to SPS. The longer processing and/or holding time and higher processing temperature can damage the structure and morphology of CNTs and this leads lack of reinforcing effects of CNTs.

As it is emphasized, almost all properties including microstructural, mechanical, electrical and thermal properties of CNT-reinforced composites depend strongly on the processing route. The processing type controls the distribution and stability of CNTs. For this reason, densification route and properties of CNT-reinforced ceramics should be considered together.

Raman spectroscopy is one of the most sensitive and reliable method to analyse the structure and characteristics of CNTs. Raman spectroscopy is also used to yield information about purity, carbonaceous impurities, defects, defect density, tube alignment, heterogeneities in CNT distribution, determination of the diameter of CNTs, etc. [23].

A typical Raman spectrum of single-wall carbon nanotubes (SWCNTs) involves four main regions. The first region belongs to low frequency peak (< 200 cm^{-1}), which originates from the radial breathing mode (RBM). RBM is inversely proportional to the tube diameter and unique for tubes having fewer walls such as single-wall or double-wall carbon nanotubes. So, it is not possible to observe RBM when the tube diameter is greater than 2 nm [23, 24]. The second region around 1340 cm^{-1} is D-band and composed of a group of peaks. D-band mainly reflects the defects and level of structural disorders (e.g. carbonaceous impurities, amorphous carbon particles, etc.) [23, 25]. Another group of peaks around 1550–1600 cm^{-1} represents G-band. G-band of a SWCNT consists of two main contributions as G^+ and G^- at around 1590 cm^{-1} and 1572 cm^{-1}, respectively [26]. The position of the G^- is sensitive to the tube diameter and expected to decrease with decreasing nanotube diameter [27]. On the other hand, the frequency of G^+ does not change with tube diameter because it corresponds to atomic displacements along the tube axis. G´-band (also known as 2D or D*) at 2600-2700 cm^{-1} ranges is an overtone mode of D-band. Compared to D-band, G´-band exhibits less sensitivity to length of nanotubes [23].

The typical Raman spectrum for multi-wall carbon nanotubes (MWCNTs) is similar to that of SWCNT. However, RBM mode does not exist and D-band is broadened in Raman spectrum of MWCNTs [23].

In most applications, the shape and intensity of peaks, as well as intensity ratio of G-band to D-band are used to indicate the defects, disorders, defect density, purity of nanotubes, crystallinity, etc. The measured results in our previous [13] study indicate that although the CNTs have some structural defects, the integrity of CNTs are maintained in the spark plasma sintered zirconia toughened alumina composites at 1400 ℃ under 40 MPa. This is indicated by the fact that the ratio of the D and G band intensities (I_D/I_G) is < 2 for the Al_2O_3-YSZ-CNT ternary composites. Moreover, the intensity of RBM and G-bands are widely utilized for purity evaluation of SWCNTs [23]. The D band is a signature of defects. This defect or disordered mode is observed when the lattice periodicity is broken by defects or amorphous carbon. In the presence of vacancies, grain boundaries or other types of defects, the D band appears around 1350 cm^{-1} [13, 28].

As emphasized, substantial damage (such as formation of kinks, caps or spherical carbon onions, etc.) in the original CNT structure can be detected after application of high pressure. Moreover, the temperatures and pressures that are applied during process influence the positions and intensities of the bands. Additionally, Raman spectrum of CNTs is sensitive to residual stresses that form as a result of contraction of the matrix during cooling. This effect can be detected from the position, intensity and shape of the Raman peaks [29]. Furthermore, a large transverse current (or energy) density during the SPS process might cause formation of imperfections including vacancies, interstitials, and local welds [13, 28].

In most cases, Raman spectroscopy analysis might not be sufficient enough by itself; so detailed microscopic

examination is imperative for the investigation of the above-mentioned defects. Besides, investigation of CNT distribution can also be performed using microscopical methods (high-resolution electron microscopy, atomic force microscopy, etc.) by visualization of nanotubes and defects. The scanning electron microscope (SEM), transmission electron microscope (TEM), atomic force microscope (AFM) and scanning tunnelling microscope (STM) techniques are used to characterize the structure of CNTs. High resolution or field emission SEM techniques are used for imaging synthesized CNTs or CNT-containing samples to investigate morphology and distribution of CNTs. Bridging effects, CNT pull-out, interaction between matrix grains and CNTs can be detected by using microscopical techniques. The tubular structure of CNTs can be investigated using transmission electron microscopy (TEM) [30]. TEM is also used to measure the intrinsic thermal vibrations of tubes [31]. Atomic force microscopy (AFM) is utilized to investigate diameter, length and distribution of CNTs. Moreover, the tip of AFM can be used to measure the mechanical properties of carbon nanotubes. Elastic modulus measurements are also performed by AFM [31]. Lourie and Wagner [32] measured the compressive response using micro-Raman spectroscopy, and reported Young's modulus of 2.8–3.6 TPa and 1.7–2.4 TPa for SWCNTs and MWCNTs, respectively. In addition, photoluminescence (PL, light emission techniques) is used to characterize dispersion quality of semiconducting SWCNTs.

III. CNT-REINFORCED ZIRCONIA-TOUGHENED ALUMINA (ZTA) COMPOSITES

The following materials are classified as nearly bioinert ceramics and composites:

(i) Alumina (aluminum oxide)

(ii) Zirconia (zirconium oxide)

(iii) Zirconia based composites as in two basic types: yttria stabilized tetragonal zirconia (TZP or YSZ) and magnesium oxide partially stabilized zirconia (Mg-PSZ)

(iv) Alumina based composites (e.g. reinforced with carbon nanotubes or graphene nanoplatelets)

(v) Zirconia toughened alumina composites (ZTA)

They are biocompatible, biologically inactive and possess stable physicochemical properties. More clearly, when a bioinert bioceramic implanted into the living hard tissue, it does not form chemical reactions or interfacial bonds with bone. Instead fibrous tissue capsule around the nearly bioinert implant material is formed. The nearly bioinert bioceramics substantially preserve their physical properties in the physiological environment. However, in long-term applications, tolerable chemical degradation and mechanical failure such as separation and fracture may develop at the interface of bone and bioceramics [7, 33, 34].

Considerable interest has existed in alumina based ceramics for the utilization as femoral heads in load-bearing artificial joints (hip, knee replacement prostheses, and also finger joints), artificial bone, artificial acetabulum and femur head, middle ear implants and dental implants. Alumina based ceramics are attractive materials because of their high stability in the human body, high hardness (~23 GPa), high Young's modulus (~400 GPa), high wear resistance, moderate flexure strength (~595 MPa), and good biocompatibility [13, 33-35]. However, alumina based components can fail because of their slow crack growth characteristics [13]. One of the most appropriate solutions of this problem is addition of a second phase material. The incorporation of zirconia into alumina results in the formation of zirconia-toughened alumina (ZTA) composites. Advantages of combined high hardness of alumina with highly fracture resistant yttria stabilized zirconia (YSZ) make Al_2O_3-YSZ system as an alternative choice to alumina and zirconia monolithic ceramics for structural and functional applications [7]. Moreover, another ideal solution can be incorporation of a material that can increase the fracture toughness and wear resistance significantly even at a very low content without destroying the biocompatibility. CNT with its high mechanical strength, high stiffness and toughening ability, is a good candidate for this purpose and considered as an attractive reinforcement for Al_2O_3-based ceramics.

The importance of CNTs-Al_2O_3 based composites has been recognized in several studies [13, 36-43]. Researchers have investigated the effects of CNTs addition on electrical, thermal, mechanical and microstructural properties of Al_2O_3-based ceramics. In these studies, different mixing techniques and processing routes have been employed. Moreover, CNTs have a great potential to improve electrical and thermal conductivity of ceramics due to their superior intrinsic properties. The differences in chirality and diameter of CNTs can change the electrical properties of them from conducting (metallic) to semiconducting. Individual CNTs possess superior electrical conductivity. The reported resistivity value for SWCNTs was ~ 10^{-4} Ωcm at room temperature [8]. Moreover, Sanvito et al. [44] reported that the conductivity of individual SWCNTs is most probably quantized with a value of $2G_o$ (G_o is conductance quantum and directly proportional with electronic charge). Consequently, authors asserted that electrical conductivity of SWCNTs does not depend on the diameter and length of nanotubes. Electrical conductivity of CNT-reinforced ceramic composites also depends on the type of processing. Flahaut et al. [45] synthesized Fe-Al_2O_3/CNT composites having 4.8 and 5.7 wt% CNTs and hot pressed at 1500 ℃ under 43 MPa with a holding time of 15 min. The relative density of the composites was measured as ~ 90%. The electrical conductivity of composites with 8.5 and 10 vol% CNTs were determined as 40-80 and 280-400 S/m, respectively. Authors explained that the relatively low values of electrical conductivity obtained were due to the low relative density and damaged CNT structure

as a result of exposing high sintering temperature during hot pressing. In another study, Zhan et al. [46] prepared Al_2O_3-SWCNT composites with 5.7, 10 and 15 vol% SWCNTs. Powder mixtures were spark plasma sintered at 1150-1200 ℃ for 3 min. The electrical conductivity values in this study were remarkably high and measured as 1050 and 3345 S/m for composites having 5.7 and 15 vol% SWCNTs, respectively. The authors explained these superior electrical conductivity results with retention of the integrity of SWCNTs during SPS process performed at relatively low temperature with a shorter holding time.

Similarly, the incorporation of CNTs to the ceramics affects the thermal properties. Thermal conductivity value for individual MWCNTs is 3000 W/mK. Compared to MWCNTs, isolated SWCNTs have higher conductivity ~ 6000 W/mK at room temperature. Contrary to electrical properties, three-dimensional network of CNTs and the nanotube-ceramic and nanotube-nanotube interfaces play an important role for thermal conductivity. This phenomenon can be explained on the basis of thermal boundary resistance; the nanotube-ceramic and nanotube-nanotube interfaces block phonon movement and cause scattering. Consequently, heat transport in ceramics having CNTs is restricted and resulting in lower thermal conductivity than that of the estimated [8].

The fracture toughness of ceramics reinforced with CNTs can be determined using different techniques including single edge notched (SENB), single edge V-notched beam (SEVNB), single edge pre-cracked beam (SEPB) and chevron notched beam (CNB). The American Society for Testing and Materials (ASTM) accepts the last three of them as standard test methods. In these methods, test samples are loaded under three-point or four-point flexural conditions. The true fracture toughness and flexure strength of the composites can be determined with mentioned test methods [8]. In addition, in the late 1970's, indentation technique was developed to determine the fracture toughness of ceramics by measuring the lengths of cracks emanating from four corners of Vickers indents. Some empirical equations were modelled by Lawn et al. [47] (1980), Anstis et al. [48] (1981), Niihara et al. [49] (1983) and Laugier et al. [50] (1985) by taking into account the variety of parameters including half of the average crack length (c), hardness (H_v), load (P), Young's modulus (E), half of the average diagonal length of indentation (a) and crack type (e.g. median/radial or Palmqvist). Moreover, it is worth to note that, the indentation method cannot be used as an accurate fracture toughness measurement. However, it is commonly preferred for comparing fracture toughness of ceramics or composites with relative densities of ~98% [42, 51].

The toughening mechanisms of CNTs include crack bridging, crack deflection and CNTs pull-out. Microscopic techniques are used to reveal the active toughening mechanism. The type of nanotubes is effective for toughening behaviour. For instance, ceramics having nanotubes with thinner wall thickness and larger diameter exhibit higher resistance to indentation damage [8].

Table 1 summarizes processing parameters, physical and mechanical properties of further studies. In these experiments [35-37], CNTs reinforced Al_2O_3-based ceramics were produced using pressureless sintering and hot pressing techniques.

TABLE 1 PHYSICAL AND MECHANICAL PROPERTIES OF PRESSURELESS SINTERED AND HOT PRESSED CNT-AL_2O_3 COMPOSITES

Matrix	CNT type and amount	Process type and parameters	Relative density (%)	Hardness (GPa)	Fracture toughness (MPa $m^{1/2}$)	Flexure strength (MPa)	Ref.
Al_2O_3	MW, 1, 3, 5 vol%	Pressureless sintering, 1500-1600 ℃, 1-2 h, 10 ℃/min, Argon	> 99 for 1%, 96.5 for 3%, ~ 92 for 5 %	22.3 for 1%, 17.9 for 3%, 12.6 for 5 %	4.1 for 1%, 3.5 for 3%, 3.6 for 5 %	543 for 1%, 364 for 3%, 286 for 5 %	[36]
Al_2O_3	MW, 0.15-2.4 vol%	Pressureless sintering, 1500-1700 ℃, 2 h, Argon	~ 99.0	21	4.6-5.5	270	[37]
Al_2O_3	MW, 2 and 5 wt%	Hot pressing, 1600 ℃, 40 MPa, 1 h, 10 ℃/min, vacuum	99.1	18 for 2 wt% 15 for 5 wt%	4.3 and 6.8 for 2 wt% 4.5 and 5.8 for 5 wt%	380 for 2 wt% 280 for 5 wt%	[38]
Al_2O_3	MW, 12 vol%	Hot pressing, 1500 ℃, 20 MPa, 1h, Argon	95.4	NA	5.55	314	[52]
Al_2O_3	MW, 2 wt%	Hot pressing, 1600 ℃, 40 MPa, 1h, vacuum	~ 99.0	18.2	4.3	367	[53]
Al_2O_3 (Y_2O_3-doped)	MW, 2 wt%			19.4	5.0	442	

Zhang et al. [36] performed pressureless sintering of MWCNT-Al_2O_3 composites at 1500-1600 ℃ with a holding time of 1-2 h, in argon. Authors reported that reactions between Al_2O_3 and CNTs produced gaseous species, which had a negative effect on densification. In another study, Sarkar et al. [37] studied pressureless sintering of MWCNT-Al_2O_3 composites at 1500-1700 ℃ with a holding time of 2 h, in argon atmosphere. They reported that 1700 ℃ is optimum sintering temperature to achieve the highest density (~99%) and addition of 0.3 vol% CNTs resulted in the highest hardness (21 GPa) and fracture

toughness (~5.5 MPa $m^{1/2}$) values at 1700 ℃. The authors indicated that main toughening mechanisms of CNTs as crack bridging and crack deflection. The enhanced toughening was also explained by the positive effect of improved matrix/CNT connectivity with the formation of internal bamboo morphology.

Ahmad et al. [38] studied hot pressed MWCNT-Al_2O_3 composites at 1600 ℃, in vacuum at a pressure of 40 MPa. Authors reported that the presence of CNTs at grain boundaries impeded grain boundary migration and affect densification negatively. In addition, grain size reduction and fracture mode change from inter-granular to trans-granular of Al_2O_3 were achieved with the addition of CNTs.

Fan et al. [52] prepared hot pressed MWCNT-Al_2O_3 composites at 1500 ℃, under 20 MPa in an argon atmosphere. Authors used two different methods for achieving a homogeneous CNTs dispersion. They reported that dispersion of 12 vol% MWCNTs in sodium dodecyl sulphate (SDS) solution and ultrasonic agitation for 30 min enhanced the dispersion characteristics of CNTs and improved the physical and mechanical properties of composites.

TABLE 2 PHYSICAL AND MECHANICAL PROPERTIES OF CNTS-REINFORCED SPARK PLASMA SINTERED AL_2O_3-BASED COMPOSITES

Matrix	CNT type and amount	Process parameters	Relative density (%)	Hardness (GPa)	Fracture toughness (MPa $m^{1/2}$)	Flexure strength (MPa)	Ref.
Al_2O_3	SW, 10 vol%	1150 ℃, 63 MPa, 3 min, vacuum	100	16.1	9.7	NA	[39]
Al_2O_3	MW, 5.04 wt%	1450 ℃, 100 MPa, 10 min, 100 ℃/min	84.4	9.7	5.7	NA	[40]
Al_2O_3	MW, 1 vol%	1450 ℃, 100 MPa, 5 min, 100 ℃/min	99.8	20.7	NA	NA	[41]
ZTA	SW, 0.01 and 0.1 wt%	1520 ℃, 80 MPa, 100 ℃/min	99.2 - 98.1	19.7 - 19.0	7.1 - 6.0	NA	[42]
	MW, 0.01 and 0.1 wt%		99.6 - 98.9	19.7 - 20.0	4.4 - 6.6		
ZTA	MW, 0.5, 1, 2 wt%	1400 ℃, 40 MPa, 5 min, 180 ℃/min, vacuum	98.5	17.8-16.9	5.46-4.62	591-359	[13]

Table 2 shows the physical and mechanical properties of CNTs-reinforced spark plasma sintered alumina based composites.

The effects of incorporation of carbon nanotubes (MWCNT and/or SWCNT) on mechanical properties of spark plasma sintered alumina composites have been examined in different studies. The highest value of fracture toughness referred to in the literature for Al_2O_3-based ceramics was obtained by Zhang et al. [39]. Authors reported an extremely high fracture toughness of ~ 9.7 MPa $m^{1/2}$ for spark plasma sintered 10vol%SWCNTs-Al_2O_3 composite. Wang et al. [40] synthesized CNT-Al_2O_3 nanocomposites by using chemical vapour deposition (CVD) technique and applied spark plasma sintering at 1150 and 1450 ℃ under 100 MPa. Authors reported the fracture toughness as ~ 3.3 MPa $m^{1/2}$. Moreover, researches related to the reinforcing effect of CNTs demonstrated that CNTs addition can prevent densification. Furthermore, depending on the CNT content, weak or strong cohesion with the matrix grains can occur. These studies have revealed that the improved densification behaviour and mechanical properties (e.g. fracture toughness, flexure strength, active toughening mechanisms) of alumina-based composites with CNTs additions are substantially dependent on the distribution, amount and position of nanotubes in the microstructure. In addition, the strength of the cohesion of matrix grains and the nanotubes have an important effect on the mentioned properties.

The fracture surfaces of spark plasma sintered (1400 ℃, under 40 MPa) CNT-reinforced zirconia toughened alumina (ZTA) composites [13] are shown in Fig. 1. The micrographs of the MWCNT-containing Al_2O_3-YSZ composites clearly demonstrate the individually distributed nanotubes within the zirconia toughened alumina (ZTA) matrix. The formation of wrapped or entangled nanotube clusters was not observed. As can be seen from the micrographs, nanotubes located mainly in inter-granular areas and they are presenting weak adherence between matrix grains and CNTs. A similar phenomenon regarding the position of nanotubes was reported in other studies [43, 53-55]. Moreover, SEM micrographs of the composites having 0.5% MWCNT (Fig. 1(a)) and 1 wt% (Fig. 1(b)) MWCNT reveal the wrapping and the bending of long CNTs, respectively. From SEM micrographs as shown in Fig. 1(a)-(d), conformation of CNTs to the shapes of the boundaries of the zirconia toughened alumina matrix grains can be readily observed.

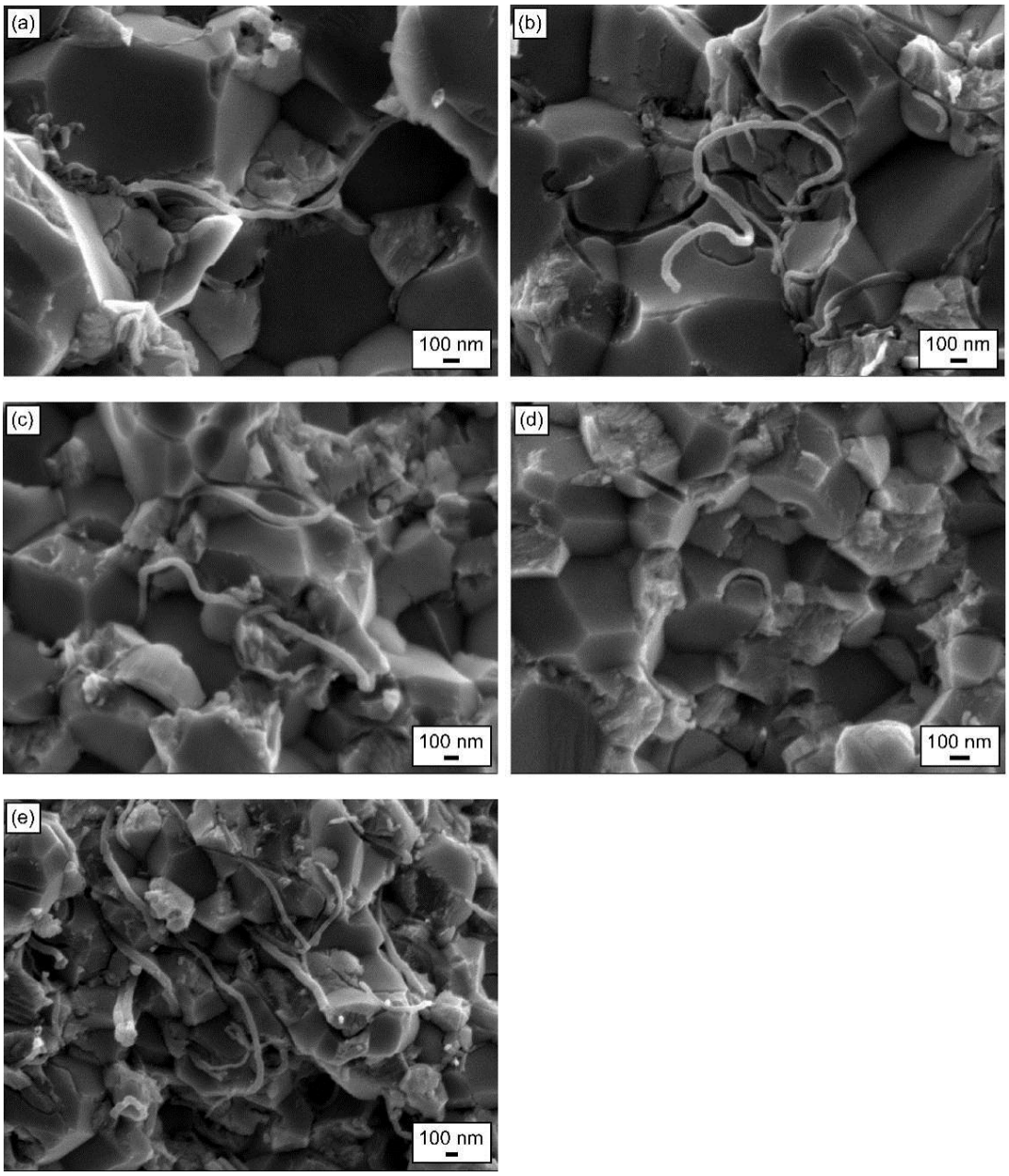

Fig. 1 SEM images of fracture surfaces of 90A10Z (vol%)-0.5CNT (wt%) (a), 90A10Z-1CNT (b), 80A20Z-0.5CNT (c), 70A30Z-0.5CNT (d), and 70A30Z-2CNT (e) ceramics sintered at 1400 ℃ for 300 s

In the same study, Vickers hardness and fracture toughness of the spark plasma sintered Al_2O_3-YSZ-MWCNT ternary composites were determined by indentation measurements. The addition of 0.5, 1 and 2 wt% CNT systematically decreased Vickers hardness of composites. More clearly, the additions of 0.5 and 2 wt% CNTs resulted in a reduction in the hardness of the 90A10Z (90 vol% Al_2O_3 and 10 vol% YSZ) composite from ~ 20.5 to ~ 19.6 and ~ 17 GPa, respectively. Similarly, an increase in the content of CNTs slightly decreased the Vickers hardness of 80A20Z (80 vol% Al_2O_3 and 20 vol% YSZ) composites. A reduction by ~ 6.5% for 1 wt% and ~ 12% for 2 wt% MWCNTs additions were observed. The slight reduction behavior in hardness was similar for 70A30Z (70 vol% Al_2O_3 and 30 vol% YSZ) composites. At 0.5, 1 and 2 wt% MWCNTs, 4, 6 and 9% declines in hardness values were detected, respectively.

The fracture toughness of the composites were also determined in the same study [13]. Measurements revealed that fracture toughness values of Al_2O_3-YSZ-CNT composites exhibited different tendency depending on the CNT content. The addition of 0.5 wt% CNTs had a little effect, 2.5, 2.7 and 1%, in increasing the fracture toughness of ZTA composites having 10, 20 and 30 vol% YSZ, respectively. However, the addition of higher amounts of CNTs (1 and 2 wt%) to ZTA matrix leaded to a reduction of fracture toughness. The indentation fracture toughness values of 90A10Z and 80A20Z composites having 2 wt% CNTs were 4.3 and 4.5 MPa $m^{1/2}$, respectively. These reported values for CNT-containing samples were ~ 11% lower than those of binary Al_2O_3-YSZ composites. Similarly, addition of 2 wt% MWCNTs to 70A30Z composite decreased the fracture toughness from ~ 5.5 to ~ 4.6 MPa $m^{1/2}$. 70A30Z composite with 0.5wt% CNTs exhibited

the highest fracture toughness, ~ 5.5 MPa $m^{1/2}$, which was almost two times that of monolithic Al_2O_3 produced under same conditions. The flexure strength values of composites having 0.5 wt% CNTs were higher than those of monolithic Al_2O_3 and Al_2O_3-YSZ binary composites. However, a considerable reduction was observed in the flexure strength values of composites having 1 and 2 wt% CNTs. With 1 wt% CNTs additions, flexure strength decreased from 558 to 469 MPa, and 589 to 490 MPa for 80A20Z and 70A30Z composites, respectively. Note that, the measured flexure strength values of composites having 2 wt% CNTs were considerably lower than those having 0.5 and 1 wt%. The measured flexure strength values exhibited composition independent behavior and remained approximately constant (~ 360 MPa) for all of the ZTA composites. Vickers hardness, fracture toughness and flexure strength results revealed that enhanced mechanical properties could be achieved with an optimum amount of CNTs addition. In addition, insufficient load bearing capacity of the grain boundaries at high MWCNTs contents can lead a reduction in mechanical properties and poor densification behavior. In that study [13], CNTs are located mainly in the inter-granular regions of the ZTA matrix grains. This causes fracture to occur along the grain boundaries and limits the toughening and strengthening contributions of CNTs.

In the biological applications, it is important to investigate the biocompatibility or toxicity of carbon nano materials. Previous studies have shown that various forms of carbon, including carbon nanotubes, carbon nanofibers (CNF) and carbon black (CB) possess a good biocompatibility. Chlopek et al. [56] investigated the biocompatibility of fibroblasts (tendon cells) and osteoblasts (bone cells) in the presence of MWCNTs. Authors reported high level of cell viability and stable osteocalcin release from osteoblasts. Smart et al. [57] prepared a detailed review about the toxicity and biocompatibility of CNTs. The authors concluded that unrefined CNTs have some degree of toxicity under both in vivo and in vitro conditions due to the existence of metal catalysts. On the other hand, the study reported that chemically functionalized CNTs have not possessed toxicity. Besides, the effect of MWCNTs on the biocompatibility of ZTA composites was reported [13]. The direct contact of human osteoblast (HOB) cells and samples was provided for 24 h to investigate the effect of composition on cell viability of HOB. Fig. 2 shows the cell viability of the samples depending on the MWCNTs content. In the same study, the effect of presence another form of carbon (i.e. carbon black) on the cell viability was also investigated. The amounts of viable cells were in the range of 94 to 99%. Preliminary cell viability studies revealed that ZTA samples having 0.5, 1 and 2 wt% CNTs and 2 wt% carbon black (CB) showed no cytotoxicity to human osteoblast (HOB) cells after 24 h of incubation.

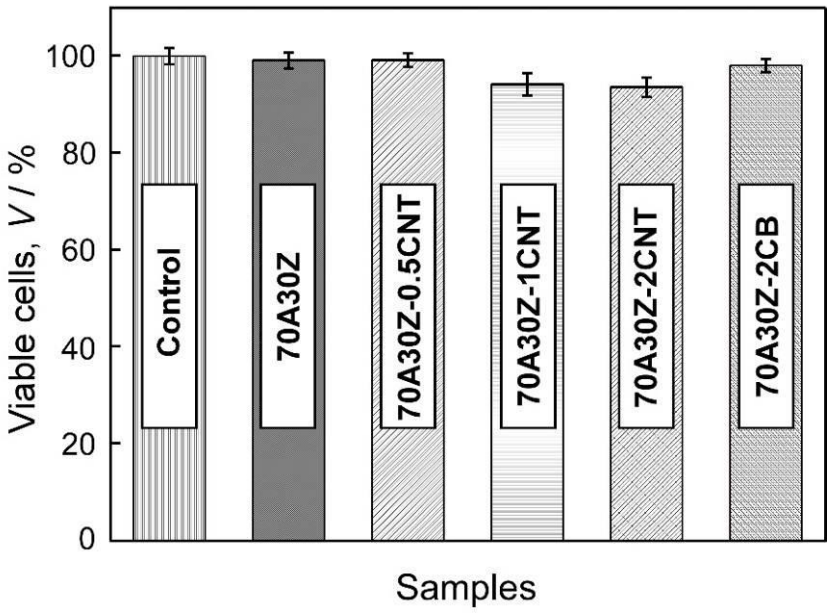

Fig. 2 Cell viability of human osteoblast cells after being cultured for a period of 24 h with 70Al2O3-30YSZ (vol%) composites having 0, 0.5, 1 and 2 wt% MWCNTs and 2 wt% CB

IV. CNT-REINFORCED ULTRA-HIGH TEMPERATURE CERAMICS (UHTC)

Ultra-high temperature ceramics and their composites are the member of non-oxide, structural advanced ceramics group. UHTCs are characterized by having a melting temperature greater than 3000 ℃ and an ability to withstand in extreme environments at high temperatures. They have high hardness (≥ 20 GPa), high thermal conductivity, good thermal shock resistance and chemical inertness [58]. The potential applications for UHTCs include use in atmospheric re-entry vehicles and hypersonic systems as nose caps and leading edges, high temperature resistant materials, corrosion resistant materials for furnaces, cathode materials for several metal processing, nozzle and armour materials and protective coating materials for hypersonic systems. The most widely used UHTCs and their basic properties are summarized in Table 3.

TABLE 3 MELTING TEMPERATURE, DENSITY, VICKERS MICROHARDNESS AND THERMAL CONDUCTIVITY DATA OF THE MOST WIDELY USED UNTCS (DC*: DECOMPOSES) [58-60]

Compound	Melting temperature (℃)	Density (g/cm^3)	Vickers microhardness (GPa)	Thermal conductivity (W/m·K, at 20℃)
HfB_2	3380	11.20	29	60
ZrB_2	3245	6.10	22.5	24.3
TiB_2	3225	4.52	22-33	24.3
NbB_2	3040	6.97	20.9	16.7
TaB_2	3040	12.54	25.6	10.9
HfC	3900	12.76	26.1	20
ZrC	3400	6.59	25.5	20,5
TiC	3100	4.94	28-35	21
NbC	3500	7.79	19.7	14.2
TaC	3800	14.50	16.7	22.1
SiC	2545-2730 (DC*, 1 atm)	3.22	24.5-28.2	α-SiC: 41 β-SiC: 43-145

ManLabs-Air Force Materials Research Laboratory (AFML) began working on the ultra-high temperature ceramics in aviation and aerospace applications in 1960s. In the early 1990s, with the development in pressure-assisted sintering techniques, researches were conducted about the utilization of intermetallic borides on leading edge and nose cap parts of hypersonic systems and atmospheric re-entry vehicles. The focus has been on hafnium diboride (HfB_2) and zirconium diboride (ZrB_2) [61, 62].

Although the superior properties possessed by the borides, due to their low fracture toughness values (< 3 MPa·$m^{1/2}$) and poor oxidation resistance, it is limited to use them alone. The performance of borides can be greatly improved by the addition of proper sintering additives and secondary phases. Silicon carbide (SiC) is the most widely used and coherent additive for boride systems to improve fracture toughness and oxidation resistance. Besides, because of providing additional toughening mechanisms, increasingly important nano scale carbon forms such as carbon nanotubes (CNTs) and graphene nanoparticles (GNPs) are also preferred reinforcing materials in the recent years.

Carbon nanotubes have been generating worldwide interest and significant attention for use in aerospace applications since 2008. In that year, NASA Ames developed an SWCNT-based chemical sensor. In 2010, NASA published a 20-year nanotechnology roadmap and explained the potential advantages of using nanostructures, particularly CNTs, in aerospace applications. In this report, the impact of nanotechnology was emphasized in four areas as follows [63, 64]:

(i) Reduced vehicle mass

(ii) improved functionality and durability

(iii) enhanced power generation, storage and propulsion

(iv) improved astronaut health management

In May 2011, Lockheed Martin revealed that the F-35 Lightning II as the first mass-produced aircraft to integrate structural nano composites (CNT-reinforced thermoset epoxy resin) in non-load bearing airframe components [63]. In August 2011, Nanocomp Technologies Inc. announced the incorporation of CNT-based sheet material (EMSHIELD) into the Juno spacecraft during its Jupiter mission in order to provide protection against electrostatic discharge (ESD). In 2013, U.S.Army declared a study in which CNTs were utilized for manufacturing high performance helicopter rotor blades. Very recently, in September 2015, NASA Langley Research Center (LaRC) has announced a proposal for their possible partners to develop additive manufacturing methods for large-scale structures with integrated functions and complex geometries provided by the incorporation of continuous CNT reinforcement.

The incorporation of CNTs has also a great potential in improving electrical and thermal conductivity, energy storage capability, electromagnetic interference shielding, recyclability, etc. [63]. In general, when the thermal conductivity of nose cap and leading edges is high enough, heat flux may be re-radiated effectively from the tip of the leading edge to the other parts of the vehicles [60]. One technique for increasing the thermal conductivity of nose cap and leading edge of hypersonic vehicles, without destroying the high temperature mechanical properties, is to add highly conductive secondary phases such as CNTs and/or GNPs.

The needs for high temperature materials that can maintain their mechanical strength and other properties at high operating temperature have driven the development of composite materials. In addition, fully dense UHTCs have been hardly obtained and required high sintering temperature and time because of strong covalent bonding and high melting temperature. Densification problem of UHTCs can be overcome by using advanced sintering techniques i.e., spark plasma sintering (SPS). Table 4 summarises the processing parameters, density results and mechanical properties of CNTs/UHTC composites reported in the literature. Hot pressing and spark plasma sintering are the most common methods, which has

been utilized to produce CNTs-reinforced UHTCs.

TABLE 4 PROCESSING PARAMETERS, PHYSICAL AND MECHANICAL PROPERTIES OF CNT-REINFORCED ULTRA-HIGH-TEMPERATURE CERAMICS (UHTC)

Matrix	CNT type and amount	Process type and parameters	Relative density (%)	Hardness (GPa)	Fracture toughness (MPa $m^{1/2}$)	Flexure strength (MPa)	Ref.
ZrB_2-SiC	MW, 2 wt%	Hot pressing, 1900 ℃, 30 MPa, 1h, vacuum	~ 96	15.5	4.6	616	[65]
ZrB_2-SiC	MW, 2.5 wt%	Hot pressing, 2000 ℃, 30 MPa, 1h, vacuum	> 99	21.7	6.1	542	[66]
C_f-SiC	MW, 1 and 2.5 wt%	Precursor infiltration and pyrolysis (PIP), pyrolyzed at 1000 ℃, 2h, Argon	90-92	NA	NA	365 for 1 wt% 210 for 2.5 wt%	[67]
SiC_f-SiC	MW, 5.3 vol%	In situ growth of CNTs	~ 90	NA	23.15	375	[68]
TaC	MW, 4 wt%	Spark plasma sintering, 1850 ℃, 100-255-363 MPa, 200 ℃/min, Argon	95-100	12.7-22.9 (nano-hardness)	1.08-1.60	NA	[69]
ZrB_2-SiC	MW, 5 wt%	Spark plasma sintering, 1750 ℃, 40 MPa, 5 min, 100 ℃/min, vacuum	99.1	23.1	4.9	214	[14]
ZrB_2	MW, 1, 5, 30 vol%	Spark plasma sintering, 1700-1750 ℃, 40 MPa, 5 min, 100 ℃/min, vacuum	97.0	15 GPa for 1 and 5 vol%, 9.7 for 30 vol%	3.6-4.1	280-426	
ZrB_2	MW, 2, 4, 6 vol%	Spark plasma sintering, 1900 ℃, 70 MPa, 15 min	95 for 2 vol%, 99 for others	14.1-16.4	1.5-3.5	150-315	[70]
ZrC-TiC	MW, 0.25-1 wt%	Spark plasma sintering, 1750 ℃, 40 MPa, 5 min, 100 ℃/min, vacuum	98.5	20-21	4.2-5	NA	[15]
ZrC-SiC	MW, 0.25-1 wt%	Spark plasma sintering, 1750 ℃, 40 MPa, 5 min, 100 ℃/min, vacuum	99.0	21.6-20.2	5.8-5.2	NA	[16]

The most of these studies aim to increase fracture toughness and flexure strength of the ceramic matrices. For instance, Tian et al. [65] prepared ZrB_2-SiC-CNT composite by hot pressing. They reported that sintering at 1900 ℃ under 30 MPa for 1h reached a low densification (~ 96%) with moderate Vickers hardness and fracture toughness values. However, a significant improvement in flexure strength was achieved. Yang et al. [66] reported that the fracture toughness in hot pressed ZrB_2-SiC composites with 2.5 wt% CNTs was almost 1.5 times higher than that of ZrB_2-SiC binary composite. The addition of 2.5 wt% CNTs led to a 22% increase in flexure strength. It was found that the CNTs formed an intragranular structure and promoted grain refinement. Wang et al. [67] prepared continuous CNTs network in carbon fiber (C_f)-SiC composite. They used precursor infiltration and pyrolysis (PIP) process assisted by freeze-drying method. The results showed a 28% increase in flexure strength at 1 wt% CNTs addition. Moreover, authors reported that further addition of CNTs, 2.5 wt%, reduced the flexure strength and density due to lack of precursor impregnation.

Exceptional tough SiC_f-SiC composite having 5.31 vol% CNTs was produced by Sun et al. [68]. Authors used three-dimensional SiC fiber preform with 30 vol% fiber content. For homogeneous CNTs dispersion, authors applied the in situ chemical vapour deposition (CVD) growth of CNTs on SiC fiber surfaces. Sun et al. [68] claimed that the flexure strength and fracture toughness in CNTs-containing sample were two times higher than that of sample without CNTs.

Bakshi et al. [69] prepared TaC-MWCNT composites using SPS at 1850 ℃ under high pressures of 100, 255 and 363 MPa. They investigated the length effect of MWCNTs (i.e. short and long CNTs have lengths of 1-3 μm and 10-20 μm, respectively) on densification, microstructure, nano-hardness and fracture toughness. Authors reported that application of high SPS pressure (255 and 363 MPa) damaged the cylindrical structure of CNTs and altered them to graphite. From mechanical characterization results, it can be inferred that, addition of longer CNTs increased nano-hardness, fracture toughness and elastic modulus values of TaC.

The ternary ZrB_2-SiC-CNT composites were prepared by the authors of this chapter and 99% relative density was achieved by SPS at 1750 ℃ under 40 MPa with a holding time of 5 min. Compared to ZrB_2-SiC binary composite, a significant difference was not observed in densification behaviour by the presence of 5 wt% CNTs. Shrinkage started below 1400 ℃ and completed at ~ 1730 ℃ for both binary and ternary composites having same amount of ZrB_2 (60 wt%). Fig. 3 shows the SEM image of the fractured surface of ZrB_2-35SiC-5CNT (in wt%) composite.

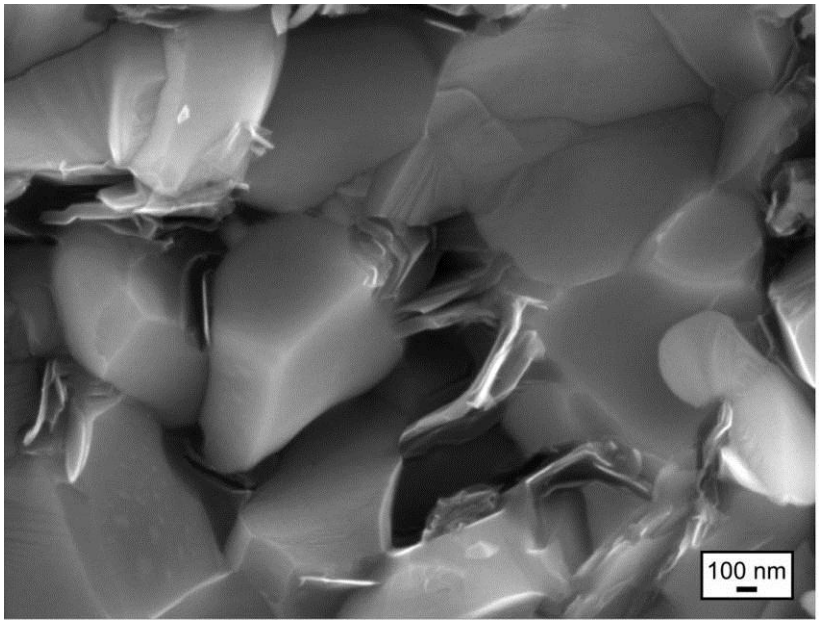

Fig. 3 SEM images of fracture surfaces of ZrB_2-SiC-CNT composite with 35 wt% SiC and 5 wt% MWCNT sintered at 1750 ℃ for 5 min

Homogeneously distributed CNTs aligned perpendicular to the crack direction and formed bridges between matrix grains. This bridging effect of CNTs increased fracture toughness by about 23% from 4 to 4.9 MPa $m^{1/2}$. Similar bridging effect of CNTs was reported by Sun et al. [17] for alumina grains. They achieved a fracture toughness of 4.9 MPa $m^{1/2}$ with only 0.1 wt% CNTs for Al_2O_3-CNT composite.

The addition of CNTs to ZrB_2 was also studied in different studies [14, 70]. CNT-ZrB_2 composites having 1, 5 and 30 vol% MWCNTs were prepared by SPS at 1700-1750 ℃ under 40 MPa. The densification of the specimens during sintering process was evaluated by the displacement of punch rods due to the shrinkage of the samples. The additions of 1 and 5 vol% CNTs exhibited similar behaviour on densification. However, the addition of 30 vol% CNTs increased the completion temperature of shrinkage from 1700 to 1750 ℃. A relative density of ~ 97.5 was achieved for ZrB_2-MWCNTs composites.

Samples having different CNT content were heated by the flame from an oxyacetylene torch (ASTM E 285-80: ASTM Standard Test Method for Oxyacetylene Ablation Testing of Thermal Insulation Materials) that directly hit on the outer surface of the sample at heat fluxes in the range of 4000-4500 kW/m^2 for 20 s. Dynamic heat flux performance of samples was determined by observing the sample condition before and after test. Test was applied for samples having 1, 5 and 30 vol% CNTs, but sample with 30 vol% CNTs was the only one that withstand the flame for 20 s without breaking. The image of the sample just after dynamic heat flux test is given in Fig. 4.

Fig. 4 Image of ZrB_2-CNT composite with 30 vol% CNT sintered at 1750 ℃ for 5 min after dynamic heat flux test (sample diameter: 5 cm, sample thickness: 5 mm)

The effect of CNT addition on mechanical and microstructural properties of ZrC-TiC and ZrC-SiC composites was investigated [15, 16]. For understanding the effect of CNT addition, different amounts of CNTs (0.25-1 wt%) were distributed into binary composites of 80ZrC–20TiC (in vol%). Spark plasma sintering process was carried out at 1750 ℃ under 40 MPa with a 5 min holding time in vacuum. Authors reported that, the addition of 1 wt% CNTs reduced the sintering temperature required to achieve full densification from 1800 to 1750 ℃. The enhanced densification behaviour of carbides with the addition of carbon black or CNTs is possible as a result of the removal of surface oxide layers on the powders and eventuated in promoted surface diffusion.

The hardness measurement results revealed that addition of 0.25 wt% MWCNTs slightly decreased the hardness of ZrC-TiC composite from 22 to 21 GPa, and when the amount of second reinforcing phase (MWCNTs) increased, hardness results continued to decrease. This could be related to the agglomeration of CNTs. On the other hand, the fracture toughness of ZrC–TiC composites were not high as expected. The possible spinodal decomposition might affect the structure and make the system more brittle. Authors reported that, the addition of MWCNTs as second reinforcing phase improved fracture toughness. The addition of 0.5 wt% CNTs successfully increased the fracture toughness about 43% from 3.5 to 5 MPa $m^{1/2}$ in the composite containing 20 vol% TiC. Further addition of CNTs resulted in lower mechanical properties due to the agglomeration problem.

The addition of both SiC (30 vol%) and CNTs (0.25-1 wt%) as reinforcing phases for ZrC was also studied [16]. Sintering experiments were conducted in SPS system at 1750 ℃ for 5 min with a heating rate of 2.5 ℃/s in vacuum. Densification of ZrC with SiC and CNTs was successful, and 99% relative density was obtained. The grain growth of ZrC was suppressed by the addition of 10 vol% SiC and further addition of SiC (20 and 30 vol%) inhibited growth of ZrC grains. The highest hardness value (21.6 GPa) was achieved with the addition of 30 vol% SiC and 0.25 wt% MWCNTs. The fracture toughness of ZrC increased from 3.3 to 5.5 MPa $m^{1/2}$ with the addition of 30 vol% SiC.

A noticeable increase in toughness of ZrC was achieved with the addition of SiC and CNTs as reinforcing phases due to their bridging effects as shown in Fig. 5. The crack had a tendency to take place along the ZrC grains. In the SiC and CNT phases, the crack propagated along the grain boundaries and deflected at an angle (as shown by white arrows). According to the crack deflection model, the energy consumption increased with increasing deflection sites. Therefore, the crack deflecting effects of SiC and CNT could be responsible for the higher fracture toughness of ZrC-based binary and ternary composites. These studies [15, 16] indicated that, the combination of maximum relative density, hardness and fracture toughness was achieved with the additions of 0.25 and 0.50 wt% MWCNTs. Compared to TiC and CNT additions, incorporation of single phase SiC and combination of SiC and CNT improved the fracture toughness (~ 60%) of ZrC-based ceramics.

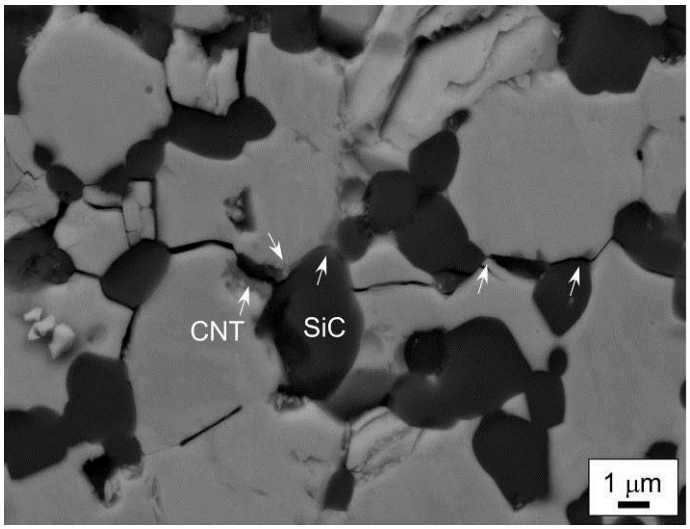

Fig. 5 SEM image of the crack propagations of ZrC-SiC composites having 1 wt% MWCNTs

Although boron carbide (B_4C) is not an ultra-high temperature ceramic, it is very promising material for a wide range of potential applications due to its high hardness (30 GPa), high wear resistance, good chemical inertness to corrosive environment and low density (2.52 g/cm^3). Goller et al. [71] investigated the effects of particle size of starting powder and MWCNTs addition on densification, microstructure and mechanical properties of B_4C. CNTs-reinforced B_4C composites (with 0.5-3 wt% MWCNTs) were sintered at 1620 and 1650 ℃, under 40 MPa in vacuum with a heating rate of 150 ℃/min by using spark plasma sintering technique. Authors reported that addition of MWCNTs reduced the completion of densification temperature about 50 ℃ compared to monolithic B_4C ceramics. Previous studies showed that the increased densification of carbides with the addition of carbon black or CNT is possible as a result of the removal of surface oxide layers (B_2O_3) on the powders and promoted surface diffusion.

In terms of mechanical properties, it was found that, the addition of 0.5 wt% MWCNTs increased the Vickers hardness of B_4C from 30.1 to 32.2 GPa. However, further increase in CNT content did not have a significant effect on hardness. Authors used the Palmqvist crack model equation for fracture toughness measurements. The addition of CNTs significantly increased the fracture toughness of B_4C specimens. The highest fracture toughness, ~ 6 MPa $m^{1/2}$, was achieved with the addition of 3 wt% CNTs to B_4C.

V. CONCLUSIONS

In the present chapter, the potential utilization of carbon nanotube reinforced ceramic composites for biological, structural and ultra-high temperature applications has been discussed. Furthermore, the chapter highlights the importance of homogeneous distribution of CNTs in ceramic matrices and stability of CNTs during densification process.

A variety of possibilities exists for the production of ceramics reinforced with carbon nanotubes (CNTs). The processing technique has a significant influence on structure, properties and performance of the final ceramic products, and accordingly, selecting the appropriate process is important to achieve the targeted properties. Spark plasma sintering (SPS) is an effective technique for achieving fully densified ceramics. In addition, CNTs can retain their original structure in the composite after SPS process; thereby successfully enhance the properties of ceramic materials.

ACKNOWLEDGMENT

The financial support for the researches in this chapter by The Scientific and Technological Research Council of Turkey (project number: 106A029), Industrial Thesis (SAN-TEZ) Projects Support Programme (project number: 00946-STZ.2011-2) and Istanbul Technical University Research Projects Division (project numbers: 32770, 35059, 36106) are greatly acknowledged. The authors wish to thank Huseyin Sezer for microstructural characterization.

REFERENCES

[1] W. D. Kingery, H. K. Bowen, and D. R. Uhlmann, *Introduction to Ceramics*, 1st ed., Singapore: John Wiley and Sons, 1960.

[2] C. B. Carter and M. G. Norton, *Ceramic Materials: Science and Engineering*, 2nd ed., New York, USA: Springer-Verlag, 2013.

[3] B. Basu and K. Balani, *Advanced Structural Ceramics*, 1st ed., New Jersey, USA: John Wiley and Sons, 2011.

[4] I. Akin, M. Li, Z. Lu, and D. C. Sinclair, "Oxygen-loss in A-site deficient $Sr_{0.85}La_{0.10}TiO_3$ perovskite," *RCS Adv*., vol. 4, pp. 32549-32554, July 2014.

[5] D. Segal, *Chemistry of Solid State Materials 1: Chemical Synthesis of Advanced Ceramic Materials*, 1st ed., Cambridge, UK: Cambridge University Press, 1989.

[6] J. Z. Shen and T. Kosmač (Eds.), *Advanced Ceramics for Dentistry*, 1st ed., USA: Elsevier, 2014.

[7] I. V. Antoniac (Ed.), *Handbook of Bioceramics and Biocomposites*, 1st ed., Switzerland: Springer International Publishing, 2015.

[8] S. C. Tjong, *Carbon Nanotube Reinforced Composites Metal and Ceramic Matrices*, 1st ed., Weinheim, Germany: Wiley-Vch Verlag GmbH&Co, 2009.

[9] J. Cho, A. R. Boccaccini, and M. S. P. Shaffer, "Ceramic matrix composites containing carbon nanotubes," *J. Mater. Sci*., vol. 44, pp. 1934-1951, 2009.

[10] I. Alig, P. Potschke, D. Lellinger, T. Skipa, S. Pegel, G. R. Kasaliwal, and T. Villmow, "Establishment, morphology and properties of carbon nanotube networks in polymer melts," *Polymer*, vol. 52, pp. 4-28, 2012.

[11] R. Banerjee and I. Manna (Eds.), *Ceramic Nanocomposites*, 1st ed., Cambridge, UK: Woodhead Publishing Limited, July 2013.

[12] I. M. Low (Ed.), *Ceramic Matrix Composites: Microstructure, Properties and Applications*, North America: CRC Press, Woodhead Publishing Limited, 2006.

[13] I. Akin, "Investigation of the microstructure, mechanical properties and cell viability of zirconia-toughened alumina composites reinforced with carbon nanotubes," *J. Ceram. Soc. Jpn*, vol. 123, pp. 405-413, May 2015.

[14] I. Akin, "Production and characterization of ZrB_2 based composites prepared by spark plasma sintering (SPS)," PhD thesis, Istanbul Technical University, Istanbul, Turkey, Sept. 2010.

[15] R. B. Acicbe and G. Goller, "Densification behavior and mechanical properties of spark plasma-sintered ZrC–TiC and ZrC–TiC–CNT composites," *J. Mater. Sci*., vol. 48, pp. 2388-2393, Nov. 2012.

[16] S. Sagdic and G. Goller, "Densification behavior and mechanical properties of spark plasma sintered ZrC–SiC and ZrC–SiC–CNT Composites," *J. Aust. Ceram. Soc*., vol. 50, pp. 76-82, 2014.

[17] J. Sun, L. Gao, and W. Li, "Colloidal processing of carbon nanotube/alumina composites," *Chem. Mater*., vol. 14, pp. 5169-5172, 2002.

[18] M. Meyyappan (Ed.), *Carbon Nanotubes Science and Applications*, California, USA: CRC Press, 2005.

[19] M. N. Rahaman (Ed.), *Sintering of Ceramics*, Florida, USA: CRC Press, Taylor & Francis Group, 2007.

[20] E. A. Olevsky, W. L. Bradbury, C. D. Haines, D. G. Martin, and D. Kapoor, "Fundamental aspects of spark plasma sintering: I. experimental analysis of scalability," *J. Am. Ceram. Soc*., vol. 95, pp. 2406-2412, 2012.

[21] Z. A. Munir and D. V. Quach, "Electric current activation of sintering: a review of the pulsed electric current sintering process," *J. Am. Ceram. Soc*., vol. 94, pp. 1-19, 2011.

[22] M. Tokita, "Mechanism of spark plasma sintering," In: Miyake S, Samandi M (Eds.), Proceedings of the international symposium on microwave, plasma and thermochemical processing of advanced materials, 1st ed., JWRI, Osaka Universities, Japan, 1997.

[23] J. H. Lehman, M. Terrones, E. Mansfield, K. E. Hurst, and V. Meunier, "Evaluating the characteristics of multiwall carbon nanotubes," *Carbon*, vol. 49, pp. 2581-2602, 2011.

[24] L. Alvarez, A. Righi, S. Rols, E. Anglaret, and J. L. Sauvajol, "Excitation energy dependence of the Raman spectrum of single-walled carbon nanotubes," *Chem. Phys. Lett*., vol. 320, pp. 441-447, 2000.

[25] Y. Miyata, K. Mizuno, and H. Kataura, "Purity and defect characterization of single-wall carbon nanotubes using Raman spectroscopy," *J. Nanomater*., vol. 2011, Article ID 786763, 2011.

[26] P. Puech, E. Flahaut, A. Bassil, T. Juffmann, F. Beuneu, and W. S. Bacsa, "Raman bands of double-wall carbon nanotubes: comparison with single- and triple-wall carbon nanotubes, and influence of annealing and electron irradiation," *J. Raman Spectrosc*., vol. 38, pp. 714-720, 2007.

[27] H. Telg, J. G. Duque, M. Staiger, X. Tu, F. Hennrich, M. M. Kappes, M. Zheng, J. Maultzsch, C. Thomsen, and S. K. Doorn, "Chiral index dependence of the G^+ and G^- Raman modes in semiconducting carbon nanotubes," *ACS NANO*, vol. 6, pp. 904-911, 2012.

[28] K. E. Thomson, D. Jiang, R. O. Ritchie, and A. K. Mukherjee, "A preservation study of carbon nanotubes in alumina-based nanocomposites via Raman spectroscopy and nuclear magnetic resonance," *Appl. Phys. A Mater. Sci. Process*., vol. 89, pp. 651-654, 2007.

[29] G. B. Yadhukulakrishnan, S. Karumuri, A. Rahman, R. P. Singh, A. K. Kalkan, and S. P. Harimkar, "Spark plasma sintering of graphene reinforced zirconium diboride ultra-high temperature ceramic composites," *Ceram. Int*., vol. 39, pp. 6637-6646, Aug. 2013.

[30] A. S. Paipetis and V. Kostopoulos (Eds.), *Carbon Nanotube Enhanced Aerospace Composite Materials, A New Generation of Multifunctional Hybrid Structural Composites*, Dordrecht, Netherlands: Springer, 2013.

[31] J. M. Hilding, "Characterization and Applications of Multiwalled Carbon Nanotubes," PhD thesis, University of Kentucky, Lexington, Kentucky, USA, Jan. 2004.

[32] R. S. Ruoff, D. Qian, and W. K. Liu, "Mechanical properties of carbon nanotubes: theoretical predictions and experimental measurements," *C. R. Phys*., vol. 4, pp. 993-1008, 2003.

[33] J. A. Burdick and R. L. Mauck (Eds.), *Biomaterials for Tissue Engineering Applications A Review of the Past and Future Trends*, 1st ed., Germany: Springer-Verlag, 2011.

[34] L. L. Hench and J. Wilson (Eds.), *An Introduction to Bioceramics*, Advances Series in Ceramics, vol. 1, World Scientific Publishing Co. Pte. Ltd., 1993.

[35] I. Akin, E. Yilmaz, F. Sahin, O. Yucel, and G. Goller, "Effect of CeO_2 addition on densification and microstructure of Al_2O_3–YSZ composites," *Ceram. Int*., vol. 37, pp. 3273-3280, Dec. 2011.

[36] S. C. Zhang, W. G. Fahrenholtz, G. E. Hilmas, and E. J. Yadlowsky, "Pressureless sintering of carbon nanotube–Al_2O_3 composites," *J. Eur. Ceram. Soc*., vol. 30, pp. 1373-1380, 2010.

[37] S. Sarkar and P. K. Das, "Microstructure and physicomechanical properties of pressureless sintered multiwalled carbon nanotube/alumina nanocomposites," *Ceram. Int*., vol. 38, pp. 423-432, 2012.

[38] I. Ahmad, M. Unwin, H. Cao, H. Chen, H. Zhao, A. Kennedy, and Y.Q. Zhu, "Multi-walled carbon nanotubes reinforced Al_2O_3 nanocomposites: Mechanical properties and interfacial investigations," *Compos. Sci. Technol*., vol. 70, pp. 1199-1206, 2010.

[39] G. D. Zhang, J. D. Kuntz, J. Wan, and A. K. Mukherjee, "Single-wall carbon nanotubes as attractive toughening agents in alumina-based nanocomposites," *Nat. Mater*., vol. 2, pp. 38-42, 2003.

[40] T. Zhang, L. Kumari, G. H. Du, W. Z. Li, Q. W. Wang, K. Balani, and A. Agarwal, "Mechanical properties of carbon nanotube-alumina nanocomposites synthesized by chemical vapor deposition and spark plasma sintering," *Comp. Part A*, vol. 40, pp. 86-93, 2009.

[41] F. Inam, T. Peijs, and M. J. Reece, "The production of advanced fine-grained alumina by carbon nanotube addition," *J. Eur. Ceram. Soc*., vol. 31, pp. 2853-2859, 2011.

[42] J. Echeberria, N. Rodriguez, J. Vleugels, K. Vanmeensel, A. Reyes-Rojas, A. Garcia-Reyes, C. Dominguez-Rios, A. Aguilar-Elguezabal, and M. H. Bocanegra-Bernal, "Hard and tough carbon nanotube-reinforced zirconia-toughened alumina composites prepared by spark plasma sintering," *Carbon*, vol. 50, pp. 706-717, 2012.

[43] M. H. Bocanegra-Bernal, J. Echeberria, J. Ollo, A. Garcia-Reyes, C. Dominguez-Rios, A. Reyes-Rojas, and A. Aguilar-Elguezabal, "A comparison of the effects of multi-wall and single-wall carbon nanotube additions on the properties of zirconia toughened alumina composites," *Carbon*, vol. 49, pp. 1599-1607, 2011.

[44] S. Sanvito, Y. K. Kwon, D. Tomanek, and C. J. Lambert, "Fractional quantum conductance in carbon nanotubes," *Phys. Rev. Lett*., vol. 84, pp. 1974-1977, 2000.

[45] E. Flahaut, A. Peigney, Ch. Laurent, Ch. Marliere, F. Chastel, and A. Rousset, "Carbon nanotube-metal-oxide nanocomposites: microstructure, electrical conductivity and mechanical properties," *Acta. Mater*., vol. 48, pp. 3803-3812, 2000.

[46] G. D. Zhan, J. D. Kuntz, J. E. Garay, and A. K. Mukherjee, "Electrical properties of nanoceramics reinforced with ropes of single-walled carbon nanotubes," *Appl. Phys. Lett*., vol. 83, pp. 1228-1230, 2003.

[47] B. R. Lawn, A. G. Evans, and D. B. Marshall, "Elastic/plastic indentation damage in ceramics: the median/radial crack system," *J. Am. Ceram. Soc*., vol. 63, pp. 574-581, 1980.

[48] G. R. Anstis, P. Chantikul, B. R. Lawn, and D. B. Marshall, "A critical evaluation of indentation techniques for measuring fracture toughness: I, direct crack measurements," *J. Am. Ceram. Soc*., vol. 64, pp. 533-538, Sept. 1981.

[49] K. Niihara, "A fracture mechanics analysis of indentation-induced Palmqvist crack in ceramics," *J. Mater. Sci. Lett*., vol. 2, pp. 221-223, 1983.

[50] M. T. Laugier, "The elastic plastic indentation of ceramics," *J. Mater. Sci. Lett.*, vol. 4, pp. 1539-1541, 1985.

[51] J. J. Kruzic, D. K. Kim, K. J. Koester, and R. O. Ritchie, "Indentation techniques for evaluating the fracture toughness of biomaterials and hard tissues," *J. Mech. Behav. Biomed. Mater*., vol. 2, pp. 384-395, 2009.

[52] J. Fan, D. Zhao, M. Wu, Z. Xu, and J. Sung, "Preparation and microstructure of multi-wall carbon nanotubes-toughened Al_2O_3 composite," *J. Am. Ceram. Soc*., vol. 89, pp. 750-753, 2006.

[53] I. Ahmad, M. Islam, A. A. Almajid, B. Yazdani, and Y. Zhu, "Investigation of yttria-doped alumina nanocomposites reinforced by must,-walled carbon nanotubes," *Ceram. Int.*, vol. 40, pp. 9327-9335, 2014.

[54] F. Inam, H. Yan, T. Peijs, and M. J. Reece, "The sintering and grain growth behaviour of ceramic–carbon nanotube nanocomposites," *Compos. Sci. Technol*., vol. 70, pp. 947-952, June 2010.

[55] A. L. Vasiliev, R. Poyato, and N. P. Padture, "Single-wall carbon nanotubes at ceramic grain boundaries," *Scr. Mater*., vol. 56, pp. 461-463, Mar. 2007.

[56] J. Chlopek, B. Czajkowska, B. Szaraniec, E. Frackowiak, K. Szostak, and F. Beguin, "In vitro studies of carbon nanotubes biocompatibility," *Carbon*, vol. 44, pp. 1106-1111, 2006.

[57] S. K. Smart, A. I. Cassady, G. Q. Lu, and D. J. Martin, "The biocompatibility of carbon nanotubes," *Carbon*, vol. 44, pp. 1034-1047, 2006.

[58] H. O. Pierson (Ed.), *Handbook of Refractory Carbides and Nitrides*, New Jersey, ABD: Noyes Publication, 1996.

[59] K. Sairam, J. K. Sonber, T. S. R. Ch. Murthy, C. Subramanian, R. K. Fotedar, and R. C. Hubli, "Reaction spark plasma sintering of niobium diboride," *Int. J. Refract. Met. H*., vol. 43, pp. 259-262, 2014.

[60] N. P. Bansal (Ed.), *Handbook of Ceramic Composites*, Boston: Kluwer Academic Publishers, 2004.

[61] http://www.uhtc.cira.it/presentazioni/6.2_GMarino_CIRA.pdf.

[62] http://ntrs.nasa.gov/archive/nasa/casi.ntrs.nasa.gov/20110014335.pdf.

[63] O. Gohardani, M.C. Elola, and C. Elizetxea, "Potential and prospective implementation of carbon nanotubes on next generation aircraft and space vehicles: A review of current and expected applications in aerospace sciences," *Prog. Aerosp. Sci*., vol. 77, pp. 42-68, July 2014.

[64] M. A. Meador, B. Files, J. Li, H. Manohara, D. Powell, and E.J. Siochi (Eds.), *Nanotechnology Roadmap*, Technology Area 10, USA: NASA, Nov. 2010.

[65] W. B. Tian, Y. M. Kan, G. J. Zhang, and P. L. Wang, "Effect of carbon nanotubes on the properties of ZrB_2-SiC ceramics," *Mat. Sci. Eng. A*, vol. 487, pp. 568-573, 2008.

[66] F. Yang, X. Zhang, and J. Han, "Preparation and properties of ZrB_2-SiC ceramic composites reinforced by carbon nanotubes," *J. Inorg. Mater*., vol. 23, pp. 950-954, Sept. 2008.

[67] L. Wang, F. Hou, X. Wang, J. Liu, and A. Guo, "Preparation and mechanical properties of continuous carbon nanotube networks modified C_f/SiC composite," *Adv. Mater. Sci. Eng*., vol. 2015, pp. 1-7, 2015.

[68] K. Sun, J. Yu, C. Zhang, and X. Zhou, "In situ growth carbon nanotube reinforced SiC_f/SiC composite," *Mater. Lett*., vol. 66, pp. 92-95, 2012.

[69] S. R. Bakshi, V. Musaramthota, D. A. Virzi, A. K. Keshri, D. Lahiri, V. Singh, S. Seal, and A. Agarwal, "Spark plasma sintered tantalum carbide-carbon nanotube composite: Effect of pressure, carbon nanotube length and dispersion technique on microstructure and mechanical properties," *Mat. Sci. Eng. A*, vol. 528, pp. 2538-2547, 2011.

[70] G. B. Yadhukulakrishnan, A. Rahman, S. Karumuri, M. M. Stackpoole, A. K. Kalkan, R. P.Singh, and S. P. Harimkar, "Spark plasma sintering of silicon carbide and multi-walled carbon nanotube reinforced zirconium diboride ceramic composite," *Mat. Sci. Eng. A*, vol. 552, pp. 125-133, 2012.

[71] B. Yavas, F. Sahin, O. Yucel, and G. Goller, "Effect of particle size, heating rate and CNT addition on densification, microstructure and mechanical properties of B_4C ceramics," *Ceram. Int.*, vol. 41, pp. 8936-8944, 2015.

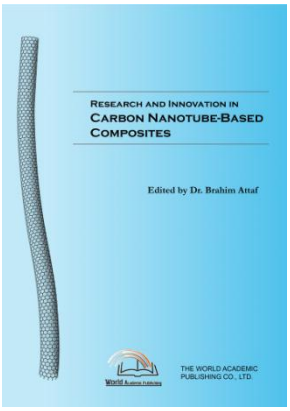

Research and Innovation in Carbon Nanotube-Based Composites
Edited by Dr. Brahim Attaf

ISBN 978-0-9889190-1-3

Hard cover, 136 pages

Publisher: The World Academic Publishing Co. Ltd.

Published in printed edition: 30, December 2015

Published online: 30, December 2015

This book of nanoscience and nanotechnology provides an overview for researchers, academicians and industrials to learn about scientific and technical advances that will shape the future evolution of composite materials reinforced with carbon nanotubes (CNTs). It involves innovation, addresses new solutions and deals with the integration of CNTs in a variety of high performance applications ranging from engineering and chemistry to medicine and biology. The presented chapters will offer readers an open access to global studies of research and innovation, technology transfer and dissemination of results and will respond effectively to challenges related to this complex and constantly growing subject area.

How to cite this book chapter

Ipek Akin and Gultekin Goller (2015). Spark Plasma Sintering of Zirconia-Toughened Alumina Composites and Ultra-High Temperature Ceramics Reinforced with Carbon Nanotubes, *Research and Innovation in Carbon Nanotube-Based Composites*, Dr. Brahim Attaf (Ed.), ISBN 978-0-9889190-1-3, WAP-AMSA, Available from: http://www.academicpub.org/amsa/